

Interactions of Divalent Metal Ions with Inorganic and Nucleoside Phosphates. 5. Kinetics of Nickel(II) with $\text{HP}_3\text{O}_{10}^{4-}$, Cytidine 5'-Triphosphate, $\text{HP}_2\text{O}_7^{3-}$, and Cytidine 5'-Diphosphate¹

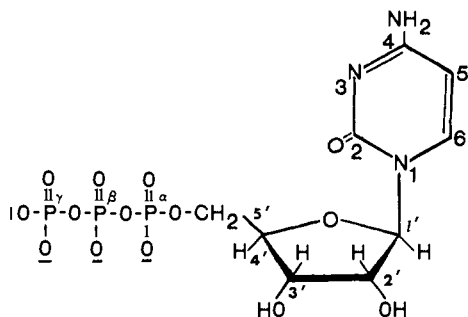
Cheryl Miller Frey and John E. Stuehr*²

Contribution from the Department of Chemistry, Case Western Reserve University, Cleveland, Ohio 44106. Received August 13, 1976

Abstract: Kinetic data are reported at 15 °C for the interaction of Ni(II) with four phosphate-containing ligands: HP_3O_{10} , CTP, HP_2O_7 , and CDP. Complexation of nickel with tripolyphosphate and pyrophosphate yields kinetic results consistent with a single rate-determining step involving the expulsion of water molecule(s) from the inner hydration shell of the nickel ion. The mechanism which quantitatively fits the data for CTP and CDP involves the formation of a 1:1 complex coupled to a 2:1 complex. In the formation of both complexes, the rate-determining step is the loss of water molecules from the nickel ion, i.e., both complexes involve inner-sphere coordination. The rate constants for the formation of the mono complexes are identical with those for the corresponding inorganic phosphates, indicating phosphate binding only. The dissociation rate constants for both Ni_2CDP and Ni_2CTP are $\sim 800 \text{ s}^{-1}$, suggesting that the binding of the second metal ion is similar in both the di- and triphosphate.

In an earlier publication from this laboratory, we reported³ the results of a temperature-jump kinetic study of the interactions of a series of di- and triphosphates with Mg(II). We found that the complexation of Mg(II) with inorganic phosphates ($\text{HP}_2\text{O}_7^{3-}$ and $\text{HP}_3\text{O}_{10}^{4-}$) yielded results consistent with a single rate-determining step involving the formation of a 1:1 complex. For complexation of magnesium with several nucleotides (ATP^{4-} , CTP^{4-} , ADP^{3-} , and CDP^{3-}), the mechanism which quantitatively fit the data involved the formation of a 1:1 complex coupled to a 2:1 complex, M_2L^6 (see mechanism c). Both adenine and cytosine nucleotides of a given charge type exhibited the same kinetic behavior with magnesium. These measurements have been summarized in a recent review.⁴

We now turn our attention to the dynamics of the analogous complexes involving Ni(II). As was found for Mg(II), stability constants for the 1:1 complex of Ni(II) with the cytosine nucleotides are, for a given charge type, identical with the stability constants for the corresponding inorganic phosphates.⁵ In addition, we find that Ni(II) forms a 2:1 complex with the cytosine nucleotides analogous to those previously reported for the Mg_2ATP and Ni_2ATP systems.^{6,7}



Ni(II) is particularly interesting in that it is now recognized to be an essential trace element in higher animals.⁸ Its roles are not yet clearly established, but the metal may be involved (e.g.) in nucleic acid metabolism.⁹ Unlike Mg(II) or Ca(II), however, Ni(II) does not generally activate nucleotides in enzyme-catalyzed reactions; it usually behaves as an inhibitor. We felt that some of the reasons for the differences in metal ion specificity might be in the mechanism of metal ion-coenzyme complex formation.

The NiHP_2O_7 and $\text{NiHP}_3\text{O}_{10}$ systems have already been

studied by temperature-jump spectrometry, but at a different temperature (25 °C) as well as in a different medium (0.1 M TMACl).¹⁰ We report new measurements in these two systems in order to have data under conditions comparable to those of the Ni-nucleotide experiments. The main reason, however, was that we wished to substantially extend the concentration range of the data for the inorganic phosphates. This is important, because kinetic data for the cytosine systems were found to deviate from linearity at relatively high concentrations.

The adenine nucleotides, which form stronger complexes with nickel, were found to display a more complicated kinetic pattern. They will be discussed in the following paper.

Experimental Section

Materials and Methods. Compounds for the kinetic experiments were prepared or purchased as described in a previous publication.³ All kinetic data were obtained at 15 °C on a temperature-jump spectrometer (Messanlagen Studiengesellschaft). The supporting electrolyte in the kinetic studies was 0.1 M KNO_3 and the pH indicator was chlorophenol red (CPR, $\text{p}K = 6.1$). The experimental solution was jumped 5 ± 0.3 °C by means of a calibrated high-voltage discharge (35 kV) and the resultant relaxation trace photographed. In all cases appropriate blanks were run to be sure that metal-ligand interactions were being measured. Proton transfer reactions of the various ligand and indicator systems were observed at 20–50 μs , but were not studied.

For the spectral measurements involving CTP and CDP, fresh stock solutions ($\sim 10^{-3}$ M) of each were made up in 0.1 M KCl (nitrate absorbs strongly in the UV). A 0.1 M stock NiCl_2 solution was prepared from reagent grade $\text{NiCl}_2 \cdot 6\text{H}_2\text{O}$ (MCB) and standardized spectrally at 395 nm with a 5-cm cell. All spectral measurements were made on a Beckman/Gilmont DU spectrophotometer; reproducibility was ± 0.002 absorbance unit.

For measurements of difference spectra of CTP and CDP at a variety of metal/ligand ratios, the following procedure was used. A set of three matched 1-cm cells contained respectively 0.1 M KCl; metal + nucleotide in 0.1 M KCl; and nucleotide in 0.1 M KCl. The 0.1 M KCl was used as a blank, and $\Delta A \equiv \text{absorbance (metal + nucleotide)} - \text{absorbance (nucleotide)}$. The different spectra for Ni-CDP and Ni-CTP were measured at 15 °C from 230 to 300 nm (Figure 1). A 10^{-2} M NiCl_2 solution was found to have negligible absorption in this region. For the nickel-cytosine nucleotides at a 1:1 ratio, the difference absorbances were very small (≈ 0.003). Solutions with ratios $\geq 20:1$ gave moderately large and reproducible readings. For measurements of the formation constant of the M_2L complex, an optimum wavelength for each system was selected and the absorbance of various metal/ligand ratios measured. The nucleotide concentrations were

Table I. Equilibrium Constants for Metal Complex and Ligand Ionization Equilibria in 0.1 M KNO_3 at 15 °C^a

Ligand	pK_{a_1}	pK_{a_2}	System	Log K_{MHL}	Log K_{ML}	$K_{M_2L}^c$
CTP	4.85	6.63	Ni-CTP	2.68	4.41	170 ± 30
$H_3P_3O_{10}^b$	5.50	7.93	Ni- P_3O_{10}	4.40	7.20	
CDP	4.56	6.38	Ni-CDP	1.87	3.48	47 ± 15
$H_4P_2O_7^b$	6.02	8.36	Ni- P_2O_7	3.50	6.22	

^a Data from ref 4 unless otherwise indicated. ^b pK_{a_i} 's refer to the last two phosphate ionizations. ^c Present measurements; see text.

typically 3×10^{-4} M and the metal ion concentration was varied at constant pH from 10 to 100 times the nucleotide concentration.

Difference spectra involving cytidine and nickel were run using two 1-cm split cells. One side of the cell contained 6×10^{-4} M cytidine in 0.1 M KCl; the other side, 0.1 M $NiCl_2$. Split cells were used because nickel solutions this high in concentration had measurable absorption in the UV.

Potentiometric titrations were carried out on a Corning 101 digital meter with a glass electrode (Fisher 13-639-3) and an Orion reference electrode (no. 90-01). A 15-mL aliquot of the substance being titrated under a nitrogen atmosphere in 0.1 M KCl was placed in a cell thermostated at 15 °C. The titrant (0.1 M HCl) was added from a 2-mL Gilmont microburet.

Treatment of Data. The analysis we used for the spectral data involving CTP and CDP is essentially that outlined by Glassman et al.⁷ The metal-nucleotide solutions can be considered an equilibrium mixture of the following species: HL, L, MHL, ML, M_2L , and M. The protonated complexes can be ignored at the pH's at which we are making measurements ($pH > 6$). As a consequence, the system can be defined by the following constants:

$$K_{ML} = \frac{(ML)}{(M)(L)} \quad K_{M_2L} = \frac{(M_2L)}{(M)(ML)}$$

Cell 1 contains the metal + nucleotide solution; therefore

$$A_1 = \epsilon_L(L) + \epsilon_{ML}(ML) + \epsilon_{M_2L}(M_2L) \quad (1)$$

and cell 2 contains just the nucleotide:

$$A_2 = \epsilon_L(L^0) \quad (2)$$

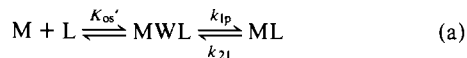
where L^0 = total concentration of the nucleotide. We can adjust our experimental conditions such that the situation $M^0 \gg L^0$ holds; therefore $M \approx M^0$. Ni-CDP and -CTP solutions have spectra virtually identical with those of the free nucleotides even when the metal is present in tenfold excess. Under these conditions, practically all the nucleotide exists in a 1:1 phosphate-bound complex. From these observations we conclude that chelation of the metal ion to the phosphate backbone alone does nothing to the ring spectrum, i.e., $\epsilon_{ML} = \epsilon_L$. Equations 1 and 2 along with the stability constants K_{ML} and K_{M_2L} can then be rearranged to yield

$$1/\Delta A = \frac{1}{\Delta\epsilon_{M_2L-L}(L^0)} + \frac{1}{\Delta\epsilon_{M_2L-L}K_{M_2L}L^0} \frac{1}{M^0} \quad (3)$$

A plot of $1/\Delta A$ vs. $1/M^0$ will yield $(\Delta\epsilon_{M_2L-L})^{-1}$ from the intercept (since L^0 is known) and $(\Delta\epsilon_{M_2L-L}K_{M_2L})^{-1}$ from the slope.

Temperature-jump kinetic data were obtained for all four systems as a function of concentration and pH. Relaxation times were computed from at least three oscilloscope traces. Reproducibility was generally $\pm 5\%$ in the relaxation times. Table I contains the various equilibrium constants used to calculate the concentrations of the individual species as well as specific concentration functions. All calculations were performed on a Univac 1108 computer.

Metal complexation reactions are generally interpreted by means of the Eigen-Tamm mechanism,¹² which describes the reactions as the rapid formation of an outer-sphere complex (MWL) followed by the rate-determining formation of the inner-sphere complex:



The presence of an outer-sphere complex MWL can in principle cause a slight curvature in plots of τ^{-1} vs. various concentration functions. For the isolated steps (a) the (slow) relaxation time is given by

$$\frac{1}{\tau} = k_{12} \frac{(\bar{M} + \bar{L})}{1 + K_{os}'(\bar{M} + \bar{L})} + k_{21} \quad (4)$$

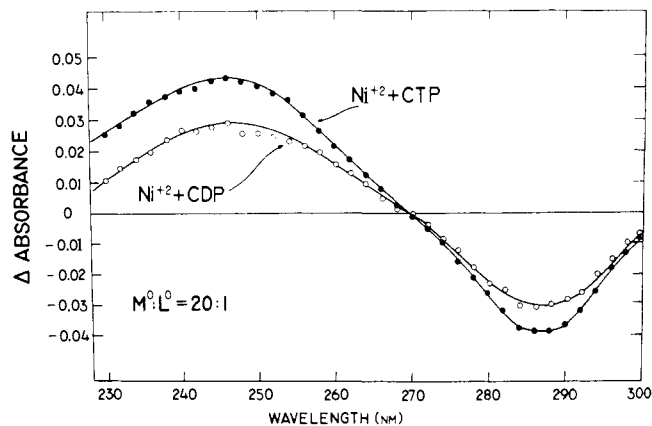


Figure 1. Differential UV absorption spectra at 15 °C for nickel with CTP and CDP in 0.1 M KCl. The CTP solution contained 3×10^{-4} M CTP and 6×10^{-3} M $NiCl_2$ at pH 6.0. The CDP solution contained 3.1×10^{-4} M CDP and 6×10^{-3} M $NiCl_2$ at pH 6.1.

where $k_{12} = K_{os}' k_{1p}$ and k_{21} is the rate constant for the dissociation of the ML complex. The values of K_{os}' needed are those (K_{os}') at 0.1 M ionic strength in the presence of a cation (K^+) which interacts with the phosphates. As described earlier, we estimate K_{os}' for the divalent metal ion interactions with di- and triphosphates to be 34 and 80, respectively.³ These values were used for the calculation of k_{1p} (ligand penetration rate constant) in Table III.

Results

Equilibrium Measurements. Spectral and potentiometric measurements were carried out on a series of cytidine solutions to see if any evidence for binding of Ni^{2+} to cytidine itself could be found. We found that, at constant pH (5.2 or 5.8), there was no discernible difference between the spectra of the mixed and unmixed solutions. Indications of a Ni^{2+} -cytidine complex were next sought via potentiometric titrations. Samples of 5×10^{-3} M cytidine were titrated as described above, alone and in the presence of a 60-fold excess of Ni^{2+} . The pH values in the presence of 0.3 M Ni^{2+} were systematically depressed (~ 0.1 unit) throughout the entire pH range (2.8–6.5). There was no systematic lowering only in the region of the ring ionization. We concluded therefore that the observed pH change was due to the increased ionic strength. Thus, we were unable to obtain any evidence for a significant interaction between Ni^{2+} and cytidine itself.

On the other hand, small but significant spectral differences were found when the cytosine nucleotides were used. Figure 1 shows the difference spectra at 15 °C for both Ni-nucleotide systems. The pH before and after mixing was kept constant to eliminate contributions from the pH dependence of the spectra of the nucleotides themselves. Even at 20:1 metal-ligand ratios the cytosine nucleotides exhibit a maximum difference of less than 0.05 unit. Plots of $1/\Delta A$ vs. $1/M^0$ (eq 3) can be found in Figure 2. The values obtained for K_{M_2L} for both systems are listed in Table I. Uncertainties are fairly large because of the small absorbance differences and difficulties in maintaining a constant pH in such dilute nucleotide solutions.

Kinetic Measurements. Inorganic Phosphates. As in previous

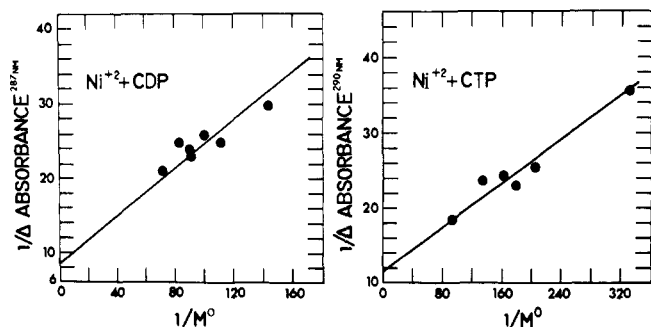


Figure 2. $1/\Delta A$ of Ni^{2+} -(CDP, CTP) vs. $1/M^0$. The concentration of CTP was 3.1×10^{-4} M in 0.1 M KCl. The pH was kept at 6.10 ± 0.05 for all points. The concentration of CDP was 3.1×10^{-4} M in 0.1 M KCl and the pH was maintained at 6.00 ± 0.05 .

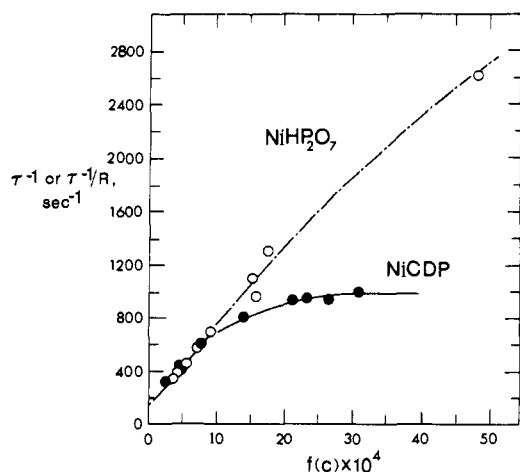


Figure 3. Dependence of τ^{-1} for NiCDP upon the concentration relationship $f(C) = \bar{M}/(1 + \beta) + \bar{L}$. For NiHP_2O_7 , $f(C) = [\bar{M} \times Q + \bar{HL}] \cdot R^{-1}$ and the ordinate is τ^{-1}/R .

studies, kinetic experiments involving triphosphosphate and pyrophosphate were run at pH values such that the predominant complexes involved the protonated species ($\text{HP}_3\text{O}_{10}^{4-}$ and $\text{HP}_2\text{O}_7^{3-}$). These species are analogous to the corresponding nucleotides in charge and phosphate binding sites. Tabulations of concentration data and relaxation times for $\text{NiHP}_3\text{O}_{10}$ and NiHP_2O_7 are given in Table II. The concentration range studied was typically $(2-5) \times 10^{-4}$ to $(3-10) \times 10^{-2}$ M. Solubility limitations prohibited kinetic measurements at higher concentrations. Measured relaxation times varied from 0.4 to 2.5 ms for the NiHP_2O_7 systems, and from 1.5 to 5 ms for $\text{NiHP}_3\text{O}_{10}$.

Relaxation time data in terms of the appropriate concentration functions for association reactions are displayed in Figures 3 and 4. Graphs for both inorganic phosphates are nearly linear over the entire concentration range investigated. This finding is consistent with the previous study¹⁰ of Ni(II) with these phosphates over a smaller concentration range at 25 °C. In addition, we had found the same behavior for the analogous reactions involving Mg(II).³ In the present work we were able to extend the concentration range for the NiHP_2O_7 system to quite high concentrations. The slight curvature shown results solely from that predicted (see eq 4) by outer sphere equilibrium constants of 34 and 80 for the di- and triphosphates, respectively. Figure 3 clearly demonstrates that the near linearity continues at concentrations where the relaxation time for the corresponding cytosine nucleotide becomes virtually concentration independent.

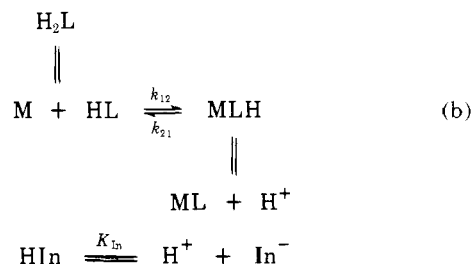
The mechanism consistent with the data for the complexation

Table II. Kinetic Data^a at 15 °C, 0.1 M KNO_3

$M^0,^b$ $M \times 10^2$	$L^0,^b$ $M \times 10^2$	pH ^c	$1/\tau^d$ (exptl), s^{-1}	$1/\tau$ (calcd), ^e s^{-1}
1. NiCTP				
0.980	0.997	6.29	1003	979
0.900	0.901	6.34	825	972
0.784	0.797	6.32	975	933
0.720	0.721	6.39	912	915
0.540	0.541	6.51	866	831
0.400	0.487	5.93	690	816
0.400	0.408	6.47	656	772
0.300	0.398	6.00	631	693
0.200	0.204	6.60	601	621
0.200	0.249	6.06	607	627
0.100	0.102	6.66	453	471
0.100	0.103	6.23	440	488
0.040	0.041	6.63	319	302
0.040	0.041	6.55	279	301
2. $\text{NiHP}_3\text{O}_{10}$				
0.750	0.784	5.84	910	
0.620	0.627	5.83	748	
0.465	0.470	5.89	460	
0.233	0.235	5.95	391	
0.078	0.078	6.07	296	
0.062	0.063	6.09	259	
0.047	0.047	6.14	229	
3. NiCDP				
1.000	1.040	6.55	1050	973
0.750	0.780	6.52	950	944
0.603	0.816	6.17	976	907
0.563	0.585	6.57	980	913
0.482	0.653	6.28	952	875
0.241	0.326	6.36	816	838
0.100	0.113	6.19	554	630
0.096	0.131	6.18	625	624
0.053	0.054	6.56	408	477
0.049	0.055	6.29	459	451
0.020	0.023	6.37	338	339
4. NiHP_2O_7				
1.000	1.540	6.40	2068	
0.582	0.794	6.25	1277	
0.490	0.802	5.85	1242	
0.582	0.794	5.89	1075	
0.512	0.552	6.24	804	
0.256	0.276	6.05	679	
0.128	0.188	5.83	511	
0.032	0.035	6.16	250	
0.016	0.017	6.32	173	

^a Kinetic data obtained with $(2-7) \times 10^{-5}$ M chlorophenol red indicator, $\lambda = 570$ nm. ^b Overall concentrations. ^c a_H values converted to C_H by $\gamma_H = 0.83$. ^d $\pm 5\%$ deviation in average of at least three traces. ^e From eq 6.

of nickel with these inorganic phosphates is the following:



where the proton transfers to the ligand and indicator (HIn) are treated as rapid preequilibria. This mechanism is identical with that utilized previously to describe the complexation of these phosphates with magnesium and nickel.^{3,10} The relaxa-

Table III. Summary of Kinetic Data for the Interaction of Nickel with Di- and Triphosphates at 15 °C, 0.1 M KNO_3 . Previously Determined Values at 25 °C in Parentheses

	Diphosphates		Triphosphates	
	Ni-CDP	Ni- HP_2O_7	Ni-CTP	Ni- HP_3O_{10}
k_{12} , $M^{-1} s^{-1}$	5.7×10^5	5.3×10^5 (2.1×10^6) ^a	1.3×10^6	1.4×10^6 (6.8×10^6) ^a
k_{21} , s^{-1}	190	170 (310) ^a	51	55 (68) ^a
K_{os}' , M^{-1}	34	34	80	80
k_{1p} , s^{-1} (calcd) ^b	1.7×10^4	1.6×10^4 (3.1×10^4)	1.6×10^4	1.7×10^4 (2.3×10^4)
K_{M_2L} (calcd) ^c = k_{23}/K_{32}	40		160	
k_{23} , $M^{-1} s^{-1}$	3.2×10^4		1.4×10^5	
k_{32} , s^{-1} ^d	800		875	
K_{os}' , M^{-1}	2		8.7	
k_{1p} , s^{-1} (calcd) ^b	1.6×10^4		1.6×10^4	

^a Data taken at 25 °C, 0.1 M TMACl, ref 10. ^b $k_{H_2O} \sim 1.5 \times 10^4$, ref 13. ^c Obtained from the computer fitting procedure; see Table I for spectrally measured values. ^d From k_{23} and K_{M_2L} .

tion time for mechanism (b) is given by

$$\tau^{-1} = k_{12} (\overline{M} \cdot Q + \overline{HL}) + k_{21} \cdot R \quad (5)$$

where Q and R are correction factors resulting from the rapid equilibria involving H_2L , ML , and the indicator.¹¹ A graph of τ^{-1}/R vs. $(\overline{M} \cdot Q + \overline{HL})/R$ yields a nearly straight line from which k_{12} and k_{21} may be obtained as the limiting slope and intercept, respectively. The slight curvature shown is that predicted by eq 4 for contributions from the outer sphere complex. The rate constants are summarized in Table III.

Cytosine Nucleotides. Concentration data and relaxation times for the NiCDP and NiCTP systems are given in Table II. Figures 3 and 4 show graphs of τ^{-1} vs. $\overline{M}/(1 + \beta) + \overline{L}$, the concentration function for a simple association mechanism (see eq 7 for definitions of symbols). One sees that the graphs are linear at low concentrations, and that the limiting slopes for the cytosine nucleotides are identical with those for the corresponding inorganic phosphates (see Table III). The intercepts are also identical with those of the corresponding inorganic phosphates. At relatively high concentrations ($f(C) [= \overline{M}/(1 + \beta) + \overline{L}] \geq 5 \times 10^{-4}$ M) the graphs for both nucleotide systems deviate substantially from linearity, eventually reaching a virtually concentration independent value. The difference in behavior between nucleotides and inorganic phosphates is seen most clearly for the diphosphates (Figure 3). The linearity of the data for Ni HP_2O_7 continues at concentrations where the values of τ^{-1} for NiCDP have become essentially concentration independent.

Thus, any kinetic interpretation of the Ni-CDP and Ni-CTP systems must be consistent with the following observations: (1) dissociation rate constants (k_{21}) are identical with those for the corresponding inorganic phosphates; (2) limiting slopes (k_{12}) are also identical with the corresponding inorganic phosphates; (3) both Ni-nucleotide systems deviate from linearity at high concentrations.

We first analyzed the nucleotide data to see if the kinetic results might be due to any number of mechanistic possibilities which we had previously studied and dismissed in our study of the Mg-nucleotide systems. Contributions from (1) a pathway involving the protonated complex MHL, (2) outer-sphere association, (3) potassium ion binding, and (4) ionic strength variations again made either negligible contributions or small contributions of the wrong functional dependence. In order to test for possible contributions from an MHL pathway, for example, we carried out near-duplicate experiments at different pH's for most of the Ni-CTP solutions studied (see Table II). There were no systematic changes in the observed relaxation times that could be attributed to the alternate

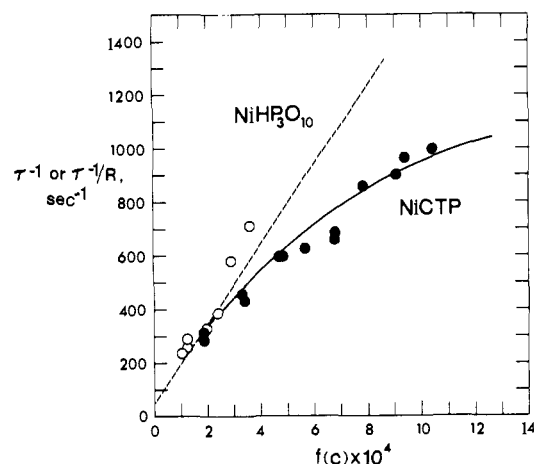
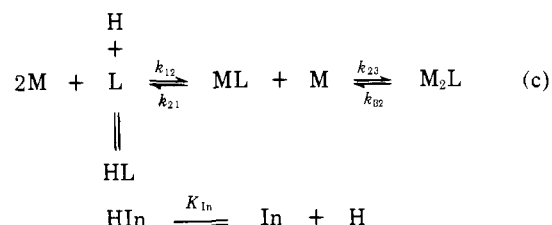


Figure 4. Dependence of τ^{-1} for NiCTP upon $f(C) = \overline{M}/(1 + \beta) + \overline{L}$. For Ni HP_3O_{10} , $f(C) = [\overline{M} \cdot Q + \overline{HL}]R^{-1}$ and the ordinate is τ^{-1}/R .

pathway. This result is consistent with the earlier observations^{3,10} that the MHL pathway was kinetically negligible above pH ~ 6 . The presence of outer-sphere complexes cannot account for the dramatic curvature observed for the Ni²⁺-nucleotide systems. This is most easily seen by comparing the behavior of the nucleotides with that of the corresponding inorganic phosphates, Figures 3 and 4. In fact, with $K_{os}' = 80$ for NiCTP, we expect a reduction of $1/\tau$ by only 8% at the highest concentration investigated. The corresponding reduction in $1/\tau$ for CDP ($K_{os}' = 34$) is $\sim 10\%$. Curvatures of this magnitude are in fact found for the inorganic phosphate systems.

On the other hand, we have already shown³ that the same concentration profile was found for the interactions of Mg(II) with these nucleotides. For the Mg(II) nucleotide systems the kinetic results were consistent with a two-step mechanism in which the complexed species were ML and M_2L . We have also demonstrated that Ni(II) forms analogous complexes with CDP and CTP (Table I). The mechanism which completely accounts for the results for NiCDP and NiCTP is



There are two coupled relaxation times associated with (c), given by

$$\frac{1}{\tau_{\pm}} = -\frac{1}{2} \left[(a_{11} + a_{22}) \pm \sqrt{(a_{11} + a_{22})^2 - 4(a_{11}a_{22} - a_{12}a_{21})} \right] \quad (6)$$

where a_{ij} are the determinantal coefficients associated with two slow steps in (c):

$$\begin{aligned} a_{11} &= -\left[k_{12} \left(\frac{\bar{M}}{1 + \beta} + \bar{L} \right) + k_{21} \right] \\ a_{21} &= k_{23}(1 + \beta)(\bar{M}\bar{L} - \bar{M}) \\ a_{12} &= (k_{12}\bar{L} - k_{21})/(1 + \beta) \\ a_{22} &= -[k_{23}(\bar{M}\bar{L} + \bar{M}) + k_{32}] \end{aligned} \quad (7)$$

and

$$\beta = \frac{H}{K_{a2} + L/(1 + \alpha)} \quad \alpha = \frac{In}{K_{In} + H}$$

The properties of the two roots to eq 6 were discussed in the earlier study.³ It is sufficient to point out here that the reciprocal of the slower of the two roots (associated with the negative sign) has two distinct types of behavior. (1) At low concentrations, τ^{-1} increases linearly with $f(C)$, with slope k_{12} and intercept k_{21} ; (2) at sufficiently high concentrations, τ^{-1} displays a much smaller slope, corresponding principally to the concentration dependence of a_{22} . This is of course the behavior we observe experimentally.

The rate constants for the two nucleotide systems were evaluated as follows. First, k_{12} and k_{21} were obtained from the low-concentration data in Figures 3 and 4. Since $k_{12}/k_{21} = K_{ML}$, there is in practice only one rate constant to be determined. The best values for these constants were found to be those for the corresponding inorganic phosphates. This is not surprising, since there is considerable overlap of the data points at low concentrations. K_{M_2L} , k_{23} , and k_{32} ($= k_{23}/K_{M_2L}$) were obtained from the high-concentration regions. In order to introduce the least amount of bias into the kinetic analysis, we treated K_{M_2L} as a variable. A large number of combinations of K_{M_2L} and k_{23} were inserted into eq 6 and the resulting predicted $1/\tau_{-}$ values were compared with the experimental values. The constants which best reproduced the data are given in Table III. The best fit constants were then used to generate the line through the points in Figures 3 and 4. We found the quality of fit to be strongly dependent on the choice of K_{M_2L} and k_{23} . For example, the best value of K_{M_2L} was 160 for the NiCTP system; a value of 180 was noticeably inferior. For both nucleotides the value of K_{M_2L} which best represented the kinetic data was well within the range of K_{M_2L} values which we obtained spectrophotometrically (Table I).

Discussion

Inorganic Phosphates. As indicated in the Results section, the data for NiHP₃O₁₀ and NiHP₂O₇ are consistent with a mechanism involving the complexed species MHL and ML. The forward rate constants (k_{12} , Table III) reflect essentially the increasing value of $K_{os'}$ with the increasing charge of the ligand. The present values of $k_{1p} \sim 1.6 \times 10^4 \text{ s}^{-1}$ are compatible with previously estimated values¹³ for the water exchange rate of nickel at the same temperature (15 °C). Rate constants agree well with the measurements of Hammes and Morrell¹⁰ when the differences in electrolyte (TMAcI vs. KNO₃) and temperature (25 vs. 15 °C) are taken into account.¹⁴

The dissociation rate constant, k_{21} , is indicative of the strength of the complex formed. As one would expect, k_{21} decreases with increasing phosphate chain length, i.e., in-

creasing number of coordination sites. Thus we can say that NiHP₃O₁₀ is kinetically about three times more stable than NiHP₂O₇.

Cytosine Nucleotides. The low-concentration data, i.e., linear portion of Figures 3 and 4 for NiCDP and NiCTP, are consistent with the reaction scheme $M + L \rightleftharpoons ML$ with $\tau^{-1} = k_{12}f(C) + k_{21}$, where $k_{12} = K_{os'}k_{1p}$. The values of k_{12} (Table III)¹⁵ again reflect only the charge on the ligand and do not show any influence of the presence of the cytosine moiety. For the same charge type, the values of the dissociation rate constant k_{21} are indistinguishable from those for the inorganic phosphates. These results indicate that the nucleoside portion of the ligand imparts negligible additional kinetic stability upon the 1:1 complex compared to just metal-phosphate chelation. The nearly identical stability constants (K_{ML}) for the nucleotides as compared to the corresponding inorganic phosphates leads to the same conclusion.

As the concentration of the reactants is increased the kinetic data for both nucleotide systems approach a plateau. This deviation from linearity is quantitatively accounted for by the coupled mechanism of the 1:1 (ML) and 2:1 (M₂L) complexes. The rate constants (k_{23}) for the formation of M₂L, listed in Table III, once more reflect only the water exchange rate of the metal and the charges on the two reacting species, ML and M. Numerically, k_{23} is determined by the $K_{os'}$ one would expect for the actual charges involved: Ni²⁺-NiCTP²⁻ and Ni²⁺-NiCDP⁻. This implies that the approaching free metal ion interacts with the charge on the ML complex as a whole. A particularly interesting finding is that the dissociation rate constant k_{32} is identical for the di- and triphosphates (800–900 s⁻¹). This suggests that the binding of the second metal ion is similar in CTP and CDP. Since the kinetics for the inorganic phosphates do not indicate the formation of the M₂L complex, the nucleoside portion of the molecule must be involved (presumably with the phosphate as well) in the binding. The fact that we could obtain difference spectra in the UV with CTP and CDP at high metal ion concentrations is indicative of binding to a ring site. In an NMR study of the Ni(II)-CTP system, Glassman et al.¹⁶ observed a slight broadening of the H-6 and H-7 ring protons at metal-ligand ratios ~1:1. However, it is unlikely that the metal ion is binding *only* to a ring position in the 2:1 complex because we could not observe any binding of cytidine and nickel either spectrally or by pH measurements (see above).

In conclusion, the dynamics of the interaction of nickel with the inorganic phosphates and cytosine nucleotides exactly parallel those reported in our earlier study with magnesium and these same systems. With either metal ion, the inorganic phosphates and the cytosine nucleotides form 1:1 complexes with the rate constants one would predict on the basis of the charge type of the ligand and the water exchange rate constant of the metal ion.

Acknowledgment. This research was supported by the National Institutes of Health in the form of a research grant (GM 13116) to J.E.S. We wish to thank Dr. Joseph Banyasz for helpful discussions.

References and Notes

- (1) A preliminary account of this work was presented at the 166th National Meeting of the American Chemical Society, Chicago, Ill., Aug 1973.
- (2) NIH Career Development Awardee (17834).
- (3) C. M. Frey, J. L. Banyasz, and J. E. Stuehr, *J. Am. Chem. Soc.*, **94**, 9198 (1972).
- (4) C. M. Frey and J. E. Stuehr "Metal Ions in Biological Systems," Vol. 1, H. Sigel, Ed., Marcel Dekker, New York, N.Y., 1974.
- (5) C. M. Frey and J. E. Stuehr, *J. Am. Chem. Soc.*, **94**, 8898 (1972).
- (6) G. A. Rechnitz, State University of New York at Buffalo, private communication.
- (7) T. A. Glassman, J. Suchy, and C. Cooper, *Biochemistry*, **12**, 2430 (1973).
- (8) W. G. Hoekstra et al., "Trace Element Metabolism in Animals", Vol. 2, University Park Press, Baltimore, Md., 1974.

- (9) F. H. Nielson and D. A. Allerich, *Fed. Proc., Fed. Am. Soc. Exp. Biol.*, **33**, 1767 (1974).
- (10) G. Hammes and M. Morrell, *J. Am. Chem. Soc.*, **86**, 1497 (1964).
- (11) $Q \equiv \frac{[K_a(ML)] + (K_M + H)K_a(1 + \alpha) \pm HL(2K_M \pm H)]}{[ML(K_a + H) + (K_M \pm H)(K_a + H)(1 + \alpha) + HL]}$; $R = \frac{[ML(K_a + 2H) \pm H((K_a + H)(1 + \alpha) \pm HL)]}{[ML(K_a + H) + (K_M + H)((K_a + H)(1 + \alpha) + HL)]}$; $\alpha = \ln/(K_{in} + H)$; $K_M = K_{ML}/(K_{MH}K_a)$. For NiHP₃O₁₀ Q ranged from 0.7 to 1.0 and R from 0.9 to 1.3; for NiHP₂O₇, $Q \sim 0.9$ to 1.2, $R \sim 0.8$ to 1.2.
- (12) M. Eigen and K. Tamm, *Z. Elektrochem.*, **66**, 93, 107 (1962).
- (13) J. W. Neely and R. E. Connick, *J. Am. Chem. Soc.*, **94**, 3419 (1972).
- (14) The earlier kinetic measurements of NiHP₃O₁₀ and NiHP₂O₇ were carried out in 0.1 M tetramethylammonium chloride. TMA⁺ binds much less, if at

- all, to the phosphate moiety; therefore k_{10} values for these two systems must be calculated with a value of $K_{os'}$ which includes only ionic strength adjustments, and not corrections for the binding of the cation of the supporting electrolyte. $K_{os'}$ can be estimated to be 70 and 300 for the di- and triphosphate, respectively. Since the value for k_{12} involves $K_{os'}$ ($k_{12} = K_{os'}k_{10}$) the forward rate constants for the two different studies of the complexation of nickel with pyro- and triphosphate will reflect the influence of the supporting electrolyte, i.e., $k_{12}(\text{TMACl}) > k_{12}(\text{KNO}_3)$.
- (15) The rate constants in Table III differ slightly from those tabulated in an earlier review (ref 4).
- (16) T. A. Glassman, C. Cooper, L. W. Harrison, and T. J. Swift, *Biochemistry*, **10**, 843 (1971).

Interactions of Divalent Metal Ions with Inorganic and Nucleoside Phosphates. 6. A Thermodynamic and Kinetic Study of the Nickel(II)-Adenosine 5'-Triphosphate and -Adenosine 5'-Diphosphate Systems

Cheryl Miller Frey and John E. Stuehr*²

Contribution from the Department of Chemistry, Case Western Reserve University, Cleveland, Ohio 44106. Received August 13, 1976

Abstract: Equilibrium binding and relaxation kinetic data are presented for the interactions of Ni(II) with ADP and ATP. Spectral measurements indicate the formation of Ni₂L complexes with both nucleotides; $K_{\text{Ni}_2\text{L}} = 40$ and 250 M^{-1} for ADP and ATP, respectively, at 15 °C and $I = 0.1$. Temperature-jump relaxation experiments, carried out over wide ranges of concentrations, were consistent with a three-step mechanism involving the formation of two 1:1 complexes (involving the phosphate moiety and phosphate plus base, respectively) and a 2:1 complex. Rate constants for the formation of the phosphate and the Ni₂L complexes were found to be similar to those for the corresponding cytosine and inorganic phosphate systems in which analogous complexes were formed. Formation of the back-bound 1:1 complex was characterized by rate constants of 450 and 1000 s^{-1} for the NiADP and NiATP systems.

A large number of enzymes require metal ions for activation, especially enzymes which utilize adenine nucleotides as cofactors.³ In such instances there is substantial evidence that the substrate is the metal-nucleotide complex and not the free nucleotide.⁴ As a consequence, considerable effort has gone into characterizing the nature of the interactions between metal ions and adenine nucleotides. Within the last decade there have been a number of studies⁵⁻¹⁰—via temperature jump spectrometry,^{6,7} NMR,⁸⁻¹⁰ UV spectroscopy,¹¹ and ORD¹²—of transition metal binding to ATP. The conclusions of these studies have been in disagreement with respect to both the duration and the site(s) of the metal-nucleotide interactions.

The major binding sites of Ni(II) with ATP are the phosphate oxygens. Using ³¹P NMR, Cohn and Hughes⁸ and Sternlicht et al.⁹ have shown that nickel binds to all three phosphate oxygens in the ML complex. They also found that the proton signals of the adenine ring were extensively broadened upon addition of Ni(II) to an aqueous (D₂O) solution of ATP (~0.1 M). From the temperature dependences of the broadening of the proton and phosphorus signals, Sternlicht et al. were able to show that the lifetimes of the metal ion in the vicinity of both the ring and the phosphate backbone were virtually identical. They concluded that in the 1:1 complex the nickel ion was bound simultaneously to the phosphate oxygens and the N₇ position in ATP.

The first temperature-jump studies of complex formation with nickel and ATP were in dilute solution (~5 × 10⁻⁴ M) and were characterized by rate constants that depended on only the charge type of the ligand and the water exchange rate of the metal ion.⁶ However, the dissociation rate constant obtained from this study was about 30 times faster than the dis-

sociation rate obtained by Sternlicht et al.^{9b} in their NMR study of Ni(II)-ATP. In order to resolve this discrepancy between temperature-jump and NMR results, Hammes and Miller⁷ reinvestigated the relaxation spectra of a number of metal ions, including Ni(II), with ATP, this time at high concentrations (0.01–0.1 M) of both metal and ligand. From extrapolation of their earlier low concentration rate data, they assumed that the previously studied time would be too fast to be observed at these high concentrations. For Ni(II)-ATP two times were observed. One time was concentration and pH dependent and was attributed to polynuclear complex formation. The second time was concentration independent, suggesting that the process was intramolecular. One likely possibility was thought to be the opening and closing of a backbound (ML') complex as represented mechanistically in Table I. Schematic representations of the 1:1 complexes are shown in Figure 1.

More recently, our studies of the complexation of Mg(II) with CTP, CDP, ATP, and ADP¹³ and Ni(II) with CTP and CDP¹⁴ have shown that the kinetic profiles obtained in these systems could be quantitatively accounted for by a mechanism involving the formation of ML and M₂L complexes (Table I). This is particularly relevant to the present study because the formation of an M₂L complex between nickel and ATP has been observed.¹⁵ Thus we are in the position of having not only a multiplicity of possible mechanisms, but also a multiplicity of complexes to consider in our analysis of the kinetic data for Ni(II)-ATP and Ni(II)-ADP. For a detailed discussion of these and other proposed mechanisms, the reader is referred to a recent review.¹⁶

We have taken several steps to maximize the amount of